Int. J. Electrochem. Sci., 4 **(2009)** 30 - 42

International Journal of
ELECTROCHEMICAL
SCIENCE
www.electrochemsci.org

On the Electrochemical Investigations of Substituted $LiNiVO_4$ for Lithium Battery cathodes

P. Kalyani[*]
Thiagarajar College of Engineering, Madurai 625 015, Tamil Nadu, India
[*]E-mail: pkalyani@tce.edu

Received: 17 September 2008 / *Accepted:* 6 November 2008 / *Published:* 20 December 2008

Three series of cation substituted $LiNiVO_4$ compounds viz., $LiNi_{1-x}Mg_xVO_4$, $LiNi_{1-x}Co_xVO_4$ and $LiNi_{1-x}Al_xVO_4$ (x=0.1, 0.3 & 0.5) have been grown by Starch-Assisted combustion (SAC) method and have been assessed for their applicability as cathode materials in rechargeable lithium batteries. Characterization by PXRD revealed phase purity of $LiNi_{1-x}Al_xVO_4$, only when x=0.0, 0.1 & 0.3 while for $LiNi_{1-x}Co_xVO_4$ and $LiNi_{1-x}Mg_xVO_4$ compounds even at x=0.5. Cyclic voltammograms establish facile Li^+ reversibility in some of these compounds. Nevertheless the phase purity aspects, electrochemical charge/discharge cycling studies at $0.1mA/cm^2$ indicate only $LiNi_{0.7}Co_{.3}VO_4$ & $LiNi_{0.7}Mg_{0.3}VO_4$ phases to have electrochemical features that may definitely be exploited for lithium battery applications.

Keywords: Lithium batteries, $LiNiVO_4$, $LiNi_{1-x}M_xVO_4$, inverse spinel and cathode materials.

1. INTRODUCTION

Lithium chemistry has evolved as a way to provide more energy in a smaller and lighter package wherein in the recent years 4V lithium-ion battery has now become a matured technology in the energy front. In the commercial lithium-ion cells, $LiCoO_2$ is the chiefly employed material as cathode for obvious reasons that it has good capacity retention, reversibility and rate capability [1] etc. But compromise is always being made with respect to excellent electrochemical performance against high cost and toxicity of $LiCoO_2$. Lithium cells with $LiMn_2O_4$ [2] and $LiNiO_2$ [3] are also widely exploited. It is to be mentioned here that $LiNiO_2$ has certain inherent problems such as, difficulty in the synthesis of stoichiometric and phase pure $LiNiO_2$ and a gradual capacity decay due to the formation of the NiO_2 phase by the phase transition of the $LiNiO_2$ structure during intercalation-deintercalation of lithium ions [4-6]. It is for these reasons that the interests of lithium battery advocates have been centered on in obtaining low cost compounds with improved electrochemical stability features.

After the introduction of the concept of *doping* to yield solid solutions (*s*ubstitution of suitable cations with appropriate atomic % at the cationic sites in the material without disrupting the basic

crystal structure and nature of the material), electrochemical investigations are being carried out with the doped analogs of the above-mentioned three candidates. For instance, a consolidated report on $LiNiO_2$ and its doped analogs can be found in [ref. 7]. Substitution even with rare-earths has been attempted, all with a view to identify economically viable and potential cathode candidates of eco-friendly nature for the future.

In 1994 Fey et al [8] observed yet another class of cubic $LiNiVO_4$ compound with inverse spinel structure to possess high voltage of ~5V. However, even with 3D-tunnels [9] (still under debate) in its crystal structure delivers only moderate discharge capacity (~90mAh/g) and with poor cyclability. The electrochemical instability during cycling has also partially been explained through opto-impedance studies made by the author of the present communication and co-workers [10, 11]. As stated earlier, cationic substitution would be a useful attempt for improving electrochemical features such as discharge capacity and cyclability of any cathode material. Hence it may be interesting to study the effects of partial cation substitution in $LiNiVO_4$ also, which formed the basis of this communication. Partial substitution at Ni sites in $LiNiVO_4$ is rarely attempted by researchers, however very few reports on Ni substitution in $LiNiVO_4$ are available [12, 13]. Therefore, the present study was aimed at investigating the effects of dopants and % of dopants like Mg and Al, in addition to Co on physical as well as electrochemical features of $LiNiVO_4$, which may likely to introduce a series of cathode active candidates for application in lithium cells. Furthermore, since there has been a constant interest towards the 5V $LiNiVO_4$ with inverse spinel structure [8], the present study involving the concept of doping at the Ni sites of $LiNiVO_4$ may assume paramount importance as of now.

In a way to identify a simple methodology to synthesize $LiNiVO_4$ sample and cation substituted analogs, a novel soft-chemical approach namely the Starch-Assisted Combustion (SAC) method has been evolved and employed for the synthesis [14]. The versatility of the newly evolved SAC method has previously been established through the synthesis and electrochemical investigation of the popular $LiCoO_2$ & $LiMn_2O_4$ compounds and the results of which have been provided in ref. [15].

In this communication, we report the synthesis and characterization of doped compounds with general formula $LiNi_{1-x}M_xVO_4$ (M=Mg, Co & Al; x=0.1, 0.3 & 0.5) obtained in a very pure state by a new inorganic synthetic procedure namely the Starch-Assisted Combustion (SAC) method. The structural properties were characterized by X-ray diffraction and vibrational spectroscopic studies which provided information on the phase purity and local environment of atoms in the crystal lattice respectively. SEM, BET surface area and particle size analysis have also been carried out. The suitability of $LiNi_{1-x}M_xVO_4$ compounds as cathode materials in rechargeable lithium batteries was tested by fabricating lithium cells in non-aqueous electrolyte and the results of the studies are discussed.

2. EXPERIMENTAL PART

A series of $LiNi_{1-x}M_xVO_4$ compounds with M= Mg, Al and Co ; x = 0.0, 0.1, 0.3 and 0.5 was synthesized by adopting Starch-Assisted Combustion (SAC) method, the procedure which has been

shown by the author of this research article to be flexible by way of synthesis of high voltage cathode materials like $LiNiVO_4$, $LiMn_2O_4$ and $LiCoO_2$ [14,15]. Starch-Assisted Combustion synthesis is a low temperature initiated and a rapid self-sustaining combustion process, which may accelerate direct conversion from the molecular mixture of the precursor solutions to the final product, without the formation of intermediate crystalline phases that require inter-diffusion for complete reaction.

In a typical synthesis, to a hot solution of "water-soluble" starch (2 g in 25 ml distilled water), crystals of nitrates of lithium (0.01 M), magnesium, aluminum nickel, cobalt (each being in the stoichiometric ratio) and ammonium meta vanadate (0.01M) were added and the solution stirred gently to ensure complete dissolution of the added salts. The resultant mixtures were oven dried at 110◦C (24h) to get the dried precursors. The dried precursors were subjected to a stepwise heat treatment to temperatures ranging from 300°C to 700°C for 3h and analyzed separately. The resultant powders of $LiNi_{1-x}M_xVO_4$ were collected and hand ground in an agate mortar and the powders subjected to physical and electrochemical characterization studies. The schematic approach of the starch-assisted route is clearly depicted in the flowchart (Fig. 1).

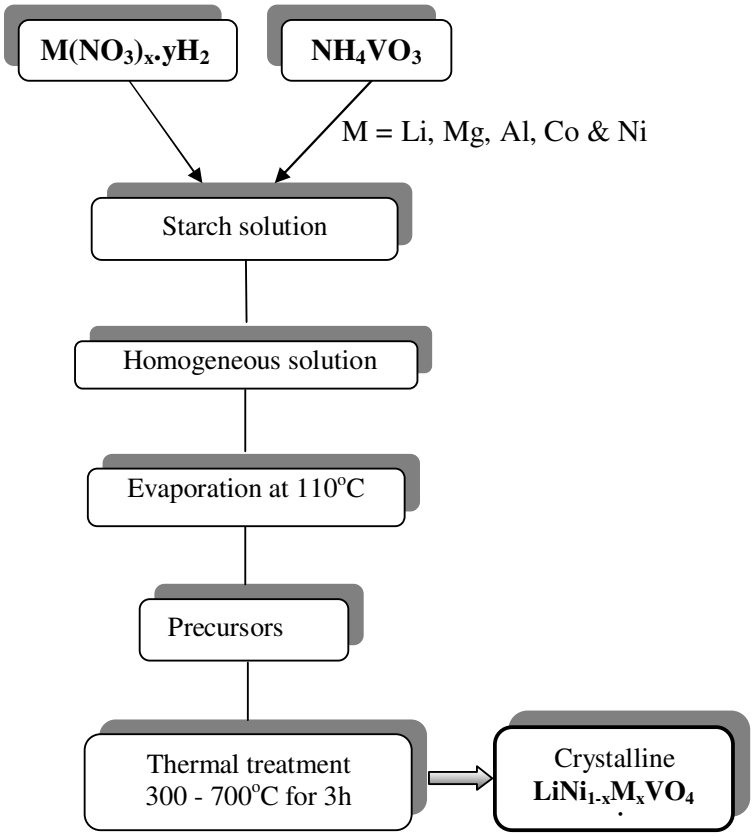

Figure 1. Steps involved in the SAC synthesis of $LiNi_{1-x}M_xVO_4$ series

Phase characterization was done by PXRD technique using JEOL-JDX 8030 X-ray diffractometer using Ni filtered Cu Kα radiation (λ = 1.5406A°) in the 2θ range of 10–70◦ at a scan rate of $0.1^{\circ}s^{-1}$. FTIR spectra were recorded with Perkin Elmer Paragon-500 FTIR Spectrophotometer using KBr pellets in the region $400cm^{-1}$ to $1000cm^{-1}$. SEMs of the samples were obtained on Hitachi S-3000 H scanning electron microscope. Surface morphology of the particles was examined from the scanning electron micrographs obtained on Hitachi S-3000 H scanning electron microscope and the particle size of the oxide materials was determined using Malvern Easy Particle sizer. Surface area of the synthesized powders was determined by BET adsorption method using low temperature nitrogen adsorption (Quanta Chrome Nova 1000, US).

Electrochemical performance of the synthesized cathode materials was evaluated by assembling cathode-limited 2016 lithium coin cells. Cathodes were fabricated by making a slurry with the cathode powders, 10% graphite and 2% PVdF as binder in *N*-methyl 2-pyrrolidone (NMP) as solvent and coating the mixture over Al foil (serves as current collector). After drying at 110◦C overnight, the discs were pressed in a hydraulic press by applying a pressure of about 10–12 kg cm^{-2} for perfect adherence of the coated material over the surface of the Al current collector. Discs of 1.6 cm diameter were punched out and typical cathodes were found to have an average active material weight of about 10–15 mg per disc. Electrolyte consisted of 1M $LiAsF_6$ dissolved in equal volumes of EC and DMC and the separator used was polypropylene cloth. Charge–discharge studies were performed using an in-house cell-testing unit. Cyclic voltammogram was recorded using 'AUTOLAB' software.

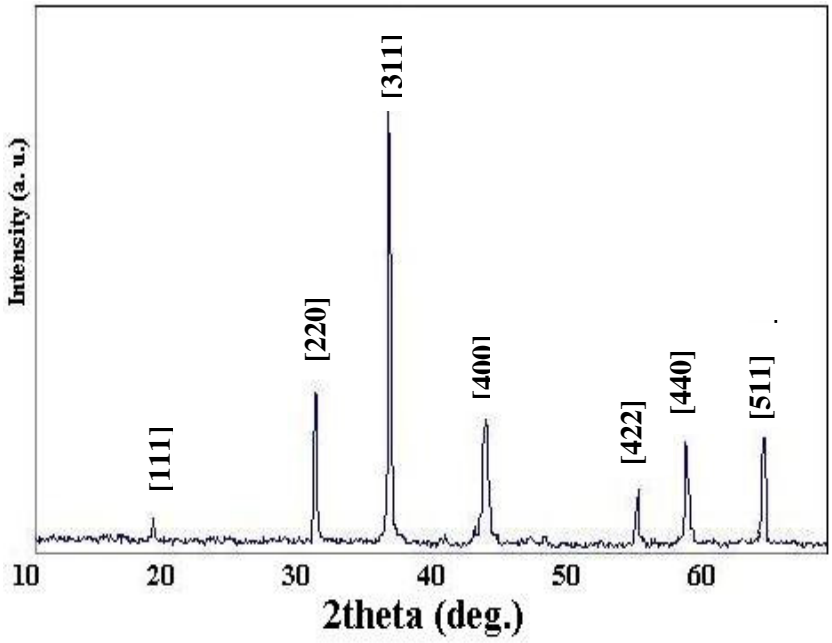

Figure 2. XRD of $LiNi_{0.7}Mg_{0.3}VO_4$.

3. RESULTS AND DISCUSSION

Typical powder x-ray diffractogram of magnesium-substituted nickel vanadates *viz.*, $LiNi_{0.9}Mg_{0.1}VO_4$ synthesized at 700°C for 3h by adopting starch-assisted combustion method is depicted in Fig.2 PXRD pattern of all the three compounds *viz.*, $LiNi_{0.9}Mg_{0.1}VO_4$, $LiNi_{0.7}Mg_{0.3}VO_4$ and $LiNi_{0.5}Mg_{0.5}VO_4$ (the latter two not shown) shows striking similarity with that of parent $LiNiVO_4$ [Fig.3 of ref. 14], thus indicating the formation of pure phase compounds with high crystalline nature. Hence it is understood that the solubility of Mg with Ni is achieved up to the substitution range selected for the study i.e. $x \leq 0.5$, proving that solid solutions could be obtained without any serious imposition on the crystal structure upon Mg dopant at least to the extent of 50%.

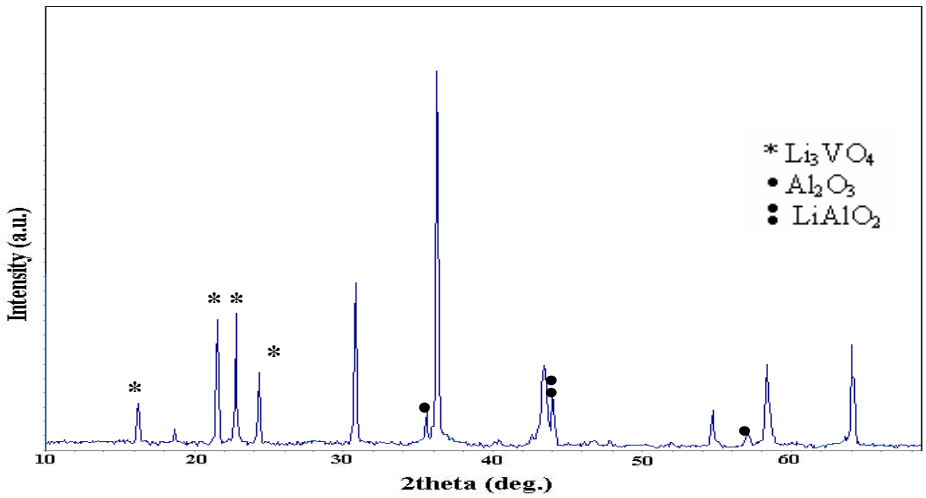

Figure 3. XRD of $LiNi_{0.5}Al_{0.5}VO_4$

A comparison of the XRD of $LiNi_{1-x}Mg_xVO_4$ (x=0.1, 0.3 and 0.5) with that of $LiNiVO_4$ (x=0) shows a decrease in $I_{(220)}/I_{(311)}$ ratio and an increase in the $I_{(311)}/I_{(400)}$ ratio. This observation may probably be attributed to the incorporation of the Mg at the Ni sites of $LiNiVO_4$ structure [16]. The crystal structure of $LiNi_{1-x}Mg_xVO_4$ (up to x=0.5) was determined to be a cubic inverse spinel having a space group *Fd-3m* in which Li, Ni and Mg ions are at *16d* O_h sites, V at *8a* T_d sites and oxygen at *32e* sites, as expected for the inverse cubic spinel structure. Progressive substitution of Ni^{2+} (0.69Å) with similar ionic size Mg^{2+} (0.66Å) influences the *"a"* and the cell volume of the doped vanadates only slightly. The crystal constants *viz.*, '*a*', and cell volume of the $LiNi_{1-x}Mg_xVO_4$ and parent $LiNiVO_4$, as determined by an iterative least squares refinement method using the indexed "*h, k, l*" values have been included in Table 1.

Similarity in PXRD pattern of $LiNi_{1-x}Co_xVO_4$ ($0.1 \leq x \leq 0.5$) compounds with that of parent $LiNiVO_4$ was observed only to show pure phase formation of all the Co-substituted derivatives with crystalline nature with out affecting the original cubic structure. As observed in the case of $LiNi_{1-x}Mg_xVO_4$ series, a decrease in $I_{(220)}/I_{(311)}$ ratio was noticed in the case of $LiNi_{1-x}Co_xVO_4$ compounds also

which is attributable to the incorporation of Co at Ni sites in the $LiNiVO_4$ structure. '*a*', and cell volume of the $LiNi_{1-x}Co_xVO_4$ compounds and that of the parent $LiNiVO_4$ are also given in Table 1.

PXRD pattern of $LiNi_{0.9}Al_{0.1}VO_4$ and $LiNi_{0.7}Al_{0.3}VO_4$ (both not shown) show striking similarity with that of the unsubstituted parent $LiNiVO_4$ compound to indicate pure phase formation and cubic inverse spinel lattice. This is also corroborated with the decrease in $I_{(220)}/I_{(311)}$ ratio with a simultaneous increase in the $I_{(311)}/I_{(400)}$ ratio when comparison is made with the pristine $LiNiVO_4$. The lattice constants *"a"* and the crystal cell volume of the $LiNi_{0.9}Al_{0.1}VO_4$ and $LiNi_{0.7}Al_{0.3}VO_4$ are found to decrease with the progressive substitution with the smaller Al^{3+} (0.51Å) for Ni^{2+} (0.69Å) and the data are provided in Table 1.

Table 1. Crystal constants and BET surface area of $LiNi_{1-x}M_xVO_4$ compounds.

Compound	Cell constants"*a*" (Å) (Unit cell volume (Å)^3)				Surface area of $LiNi_{0.9}M_{0.1}VO_4$ (g/m^2)
	x= 0.0	x = 0.1	x = 0.3	x = 0.5	
$LiNi_{1-x}Mg_xVO_4$	8.217 (554.8)	8.217 (554.8)	8.215 (554.4)	8.214 (554.2)	28
$LiNi_{1-x}Co_xVO_4$	8.217 (554.8)	8.225 (556.4)	8.241 (559.7)	8.253 (562.1)	30
$LiNi_{1-x}Al_xVO_4$	8.217 (554.8)	8.207 (552.8)	8.196 (550.6)	- -	25

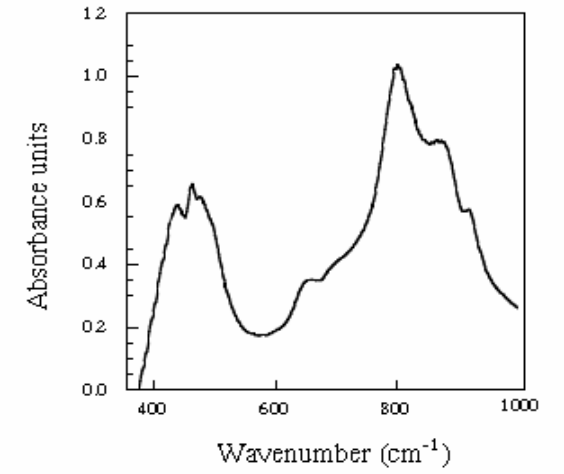

Figure 4. FT-IR spectra of Li $Ni_{0.5}Mg_{0.5}VO_4$

However, Fig. 3, which is the PXRD of $LiNi_{0.5}Al_{0.5}VO_4$, clearly shows the presence of impure phases like Li_3VO_4, $LiAlO_2$ and Al_2O_3 together with the peaks corresponding to the $LiNi_{0.5}Al_{0.5}VO_4$

phase. Hence from the PXRD studies, it may be concluded that the solubility of Al with Ni is limited to a level, probably of $0 \leq x \leq 0.3$ only, unlike $LiNi_{1-x}Mg_xVO_4$ & $LiNi_{1-x}Co_xVO_4$ where solubility of the respective substituents are viable up to 50%. Higher temperature of synthesis may result in impure phase free $LiNi_{0.5}Al_{0.5}VO_4$.

Surface area (by BET method) of one typical sample with formula $LiNi_{0.9}M_{0.1}VO_4$, representing each of the three series is also given in Table 1. The three representative samples were observed to possess almost same and high surface area indicating the smaller particle dimension of the powders achieved through the SAC method.

Fig. 4 shows the typical room temperature FT-IR spectrum of $LiNi_{0.5}Mg_{0.5}VO_4$ sample treated at 700°C. Comparison with the FT-IR spectra of the unsubstituted $LiNiVO_4$ allows one to conclude that only negligible differences exist in the peaks/band position of the magnesium substituted vanadate powders.

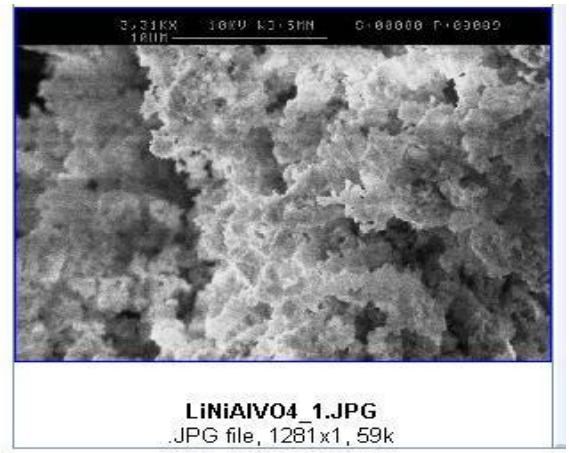

Figure 5a. SEM of $LiAl_{0.7}Ni_{0.3}VO_4$ powders

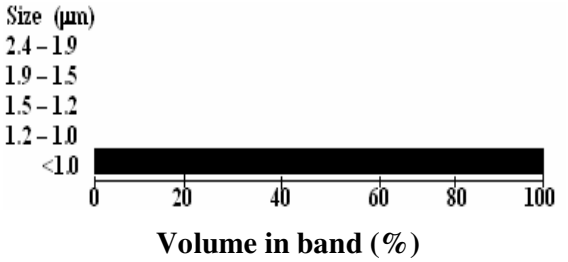

Figure 5b. Particle size distribution in $LiNi_{0.7}Al_{0.3}VO_4$

FTIR signatures observed for $LiNi_{0.5}Mg_{0.5}VO_4$ in the 400 - 750cm^{-1} region are largely associated either with the bending vibrations of the VO_4 tetrahedron or vibrations of NiO_6 and LiO_6 octahedral units in these compounds. The possible bonding of Li, Ni and probably Mg with each

oxygen atom in the VO_4 tetrahedra may bring about some asymmetry but without distorting the cubic symmetry of the fundamental unit cell. Hence broad bands around 800cm^{-1} & 850cm^{-1} are attributed to the asymmetrical stretching modes in distorted VO_4 units [17]. Also, the vibrations due to bending modes in NiO_6 octahedra i.e., ν[**M**-O-Li)] are observed around 650cm^{-1} and two weak bands around 435cm^{-1} and 410cm^{-1} may therefore be assigned to asymmetric stretching of Li-O in LiO_6 environments [18, 9]. Also, the bands in the high frequency region are assigned to the vibration between oxygen and the highest valent cation. As a result, the weak band around 900cm^{-1} is assigned to the symmetric stretching in VO_4 [9].

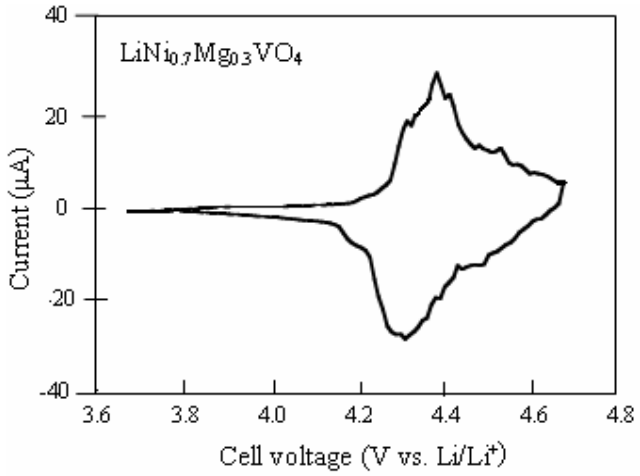

Figure 6a. Cyclic voltammogram of Li//$LiNi_{0.7}Mg_{0.3}VO_4$ cell.
Scan rate = 10μV/sec

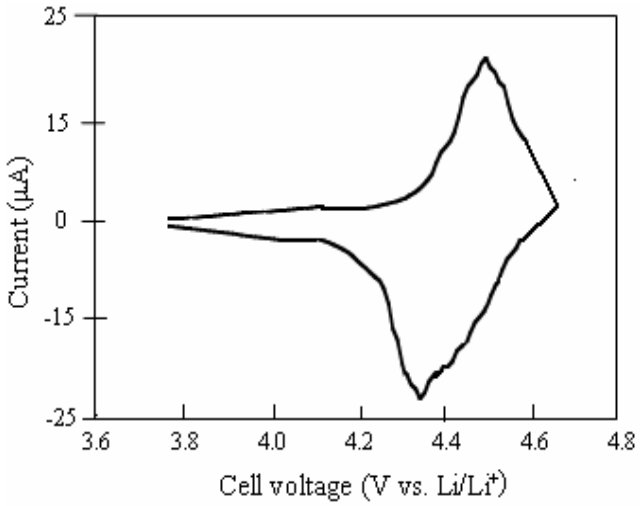

Figure 6b. Cyclic voltammogram of Li//$LiNi_{0.7}Co_{0.3}VO_4$ cell.
Scan rate = 10μV/sec

Typical SEM of $LiNi_{0.7}Al_{0.3}VO_4$ is displayed in Fig. 5a. The formation of porous and highly inter-connected mass is evidenced from SEM. It is now clear that the usage of carbonaceous fuel (starch) in SAC route coupled with medium temperature of powder processing play a vital role towards

the restricted agglomeration of particles and suppressed grain growth. Uniform distribution of reduced particle size between 1.0 & 1.2μm is obvious from the reports of laser based particle size measurements done on $LiNi_{0.7}Al_{0.3}VO_4$ material (Fig. 5b).

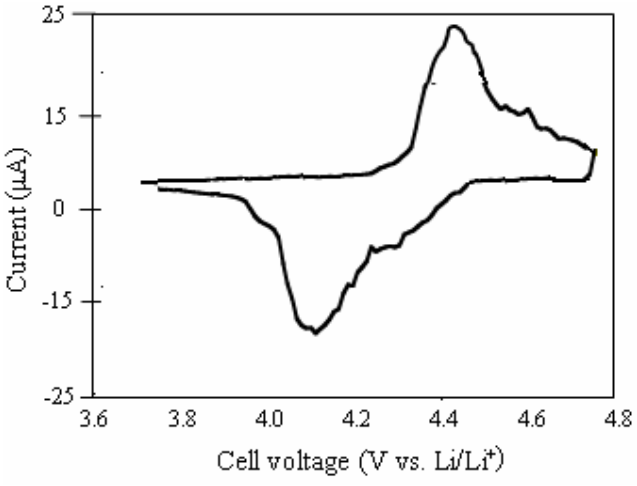

Figure 6c. Cyclic voltammogram of $Li//LiNi_{0.7}Al_{0.3}VO_4$ cell.
Scan rate = 10μV/sec

Figs. 6a, b & c respectively show the cyclic voltammogram of $Li//LiNi_{0.7}M_{0.3}VO_4$ (M=Mg, Co & Al) cells invariably recorded at a scan rate of 10μV/sec. The voltage of the forward scan has been limited to 4.7V to avoid the electrolyte decomposition, despite the usage of oxidation resistant electrolyte mixture consisting of 1M $LiAsF_6$ in equal volumes of EC and DMC.

The CV response shows the electrochemical lithium intercalation-deintercalation process of the $LiNi_{0.7}Mg_{0.3}VO_4$ electrode occurs reversibly in the range of 4.2-4.4V, (a value slightly lower than those of cobalt derivative (as evidenced in the respective CV). The CV of $Li//LiNi_{0.7}Co_{0.3}VO_4$ cells shows that the electrochemical lithium intercalation-deintercalation process occurs reversibly in the 4.35-4.5V range. The reversibility of the electrochemical process is further demonstrated by the charge-discharge cycling studies carried out with this cell.

The CV response of $Li//LiNi_{0.7}Al_{0.3}VO_4$ shows that the electrochemical lithium intercalation-deintercalation process occurs reversibly in the range of 4.1-4.4V, slightly lower than the Co-doped vanadate derivatives.

Figs.7a, b & c respectively show first charge-discharge behavior of $Li//LiNi_{0.7}Mg_{0.3}VO_4$, $Li//LiNi_{0.7}Co_{0.3}VO_4$ & $Li//LiNi_{0.9}Al_{0.1}VO_4$ cells that have been charged and discharged at a current density of $0.1mA/cm^2$ from 3V to 4.5V and Tables 2a, b & c show the variation of discharge capacity with cycle number and with the extent of respective cation substitution.

About 90mAh/g of discharge capacity is obtained for $Li//LiNi_{0.9}Mg_{0.1}VO_4$ cell during the first discharge with negligible capacity fade at the end of the 5^{th} cycle. From the Table 2a, it is obvious that the $Li//LiNi_{0.7}Mg_{0.3}VO_4$ cell exhibited a slightly higher first discharge capacity (ca. 105mAh/g) together with negligible capacity fade in the subsequent cycles. In contrast, when 50% of Mg is

present i.e. for Li//$LiNi_{0.5}Mg_{0.5}VO_4$ cell, discharge capacity was found to be lower and only an inferior electrochemical behavior was observed. Thus, a maximum of 30% of Mg substitution may be permissible to exhibit a stable and an acceptable electrochemical performance.

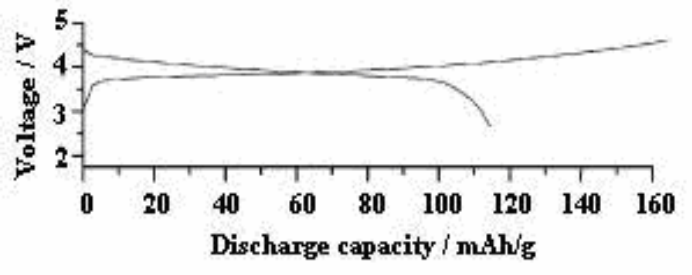

Figure 7a. Charge-discharge profile of Li//$LiNi_{0.7}Mg_{0.3}VO_4$ cell

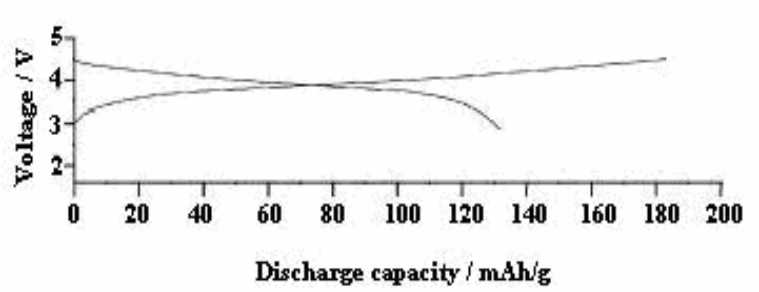

Figure 7b. Charge-discharge profile of Li//$LiNi_{0.7}Co_{0.3}VO_4$ cell

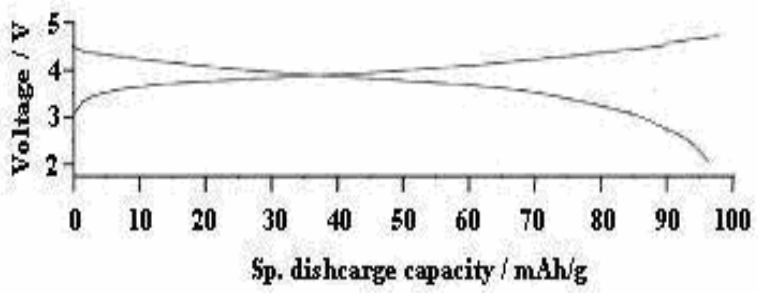

Figure 7c. Charge-discharge profile of Li//$LiNi_{0.9}Al_{0.1}VO_4$ cell

Unsubstituted $LiNiVO_4$ compound exhibited a capacity of *ca*. 90mAh/g during the first cycle, which was found to suffer from severe capacity fading problem [14]. A similar discharge capacity of around 90mAh/g was observed for $LiNi_{0.9}Co_{0.1}VO_4$, when Ni in $LiNiVO_4$ was substituted by 10% of Co, which was also found to maintain up to three cycles with a slight variation in capacity upon further cycling. On the other hand, Li//$LiNi_{0.7}Co_{0.3}VO_4$ cell exhibited a slightly higher first discharge capacity (*ca*. 120mAh/g), which showed only a minimum capacity fade over five cycles. Interestingly in $LiNi_{0.7}Co_{0.3}VO_4$, maximum capacity can be tapped between 4.5 and 3.2V region, as evidenced from Fig.7b. However, when 50% of Co was present i.e. Li//$LiNi_{0.5}Co_{0.5}VO_4$ cell showed no significant

improvement in the electrochemical features. Thus, it is understood that at least a minimum of 30% cobalt substitution may be advantageous in exhibiting a stable and acceptable electrochemical performance. Thus, the partial substitution of Ni with Co improves the electrochemical performance when compared with that of the un-substituted $LiNiVO_4$.

Table 2a. Cyclability trend of Li//$LiNi_{1-x}Mg_xVO_4$ cells.

Cycle No.	Discharge capacity of $LiNi_{1-x}Mg_xVO_4$ (mAh/g)			
	x=0.0	**x=0.1**	**x=0.3**	**x=0.5**
1	90	90	105	95
2	75	88	103	87
3	45	88	103	80
4	30	86	102	71
5	15	82	101	61

Table 2b. Cyclability trend of Li//$LiNi_{1-x}Co_xVO_4$ cells.

Cycle No.	Discharge capacity of $LiNi_{1-x}Co_xVO_4$ (mAh/g)			
	x=0.0	**x=0.1**	**x=0.3**	**x=0.5**
1	90	93	122	70
2	75	90	120	61
3	45	90	118	54
4	30	85	118	-
5	15	82	115	-

Table 2c. Cyclability trend of Li//$LiNi_{1-x}Al_xVO_4$ cells.

Cycle No.	Discharge capacity of $LiNi_{1-x}Al_xVO_4$(mAh/g)	
	x=0.0	**x=0.1**
1	90	98
2	75	98
3	45	96
4	30	95
5	15	95

About 98mAh/g of discharge capacity, which is slightly higher than that obtained for the undoped $LiNiVO_4$ was obtained for $Li//LiNi_{0.9}Al_{0.1}VO_4$ cell during the first discharge. Interestingly, the capacity retention was found to be good at least up to five cycles. But when 30% of Al is present i.e. for $Li//LiNi_{0.7}Al_{0.3}VO_4$, the observed capacity values are inferior. Thus, a maximum of 10% of Al substitution is highly advantageous to exhibit an acceptable electrochemical performance.

It may be worth mentioning here that if proper oxidation resistant electrolyte mixture is used or if the charging voltage is fixed lower than 4.5V, it would be helpful in improving the cycle life of the cells by preventing the inadvertent oxidation of the electrolyte used.

4. CONCLUSIONS

By adopting Starch-Assisted Combustion (SAC) method an unique attempt of synthesizing three series of doped derivatives of $LiNiVO_4$ viz., $LiNi_{1-x}Mg_xVO_4$, $LiNi_{1-x}Co_xVO_4$ and $LiNi_{1-x}Al_xVO_4$ (x=0.1, 0.3 & 0.5) has been made in the present study. The synthesis conditions have been facile to accommodate these cations at the Ni sites in the cubic crystal lattice. As evidenced from the PXRD studies, phase pure compounds have been obtained for $LiNi_{1-x}Al_xVO_4$ when x=0.0, 0.1 and 0.3 while for $LiNi_{1-x}Co_xVO_4$ and $LiNi_{1-x}Mg_xVO_4$ pure phase has been obtained even for x=0.5. From the present study, the maximum solubility limit of Al to yield $LiNi_{1-x}Al_xVO_4$ has been found to lie probably within 30% and for $LiNi_{1-x}Co_xVO_4$ and $LiNi_{1-x}Mg_xVO_4$ it is 50%.

Cyclic voltammogram recorded for $LiNi_{0.7}Co_{.3}VO_4$, $LiNi_{0.7}Mg_{0.3}VO_4$ and $LiNi_{0.9}Al_{0.1}VO_4$ reveal high lithium reversibility and supports for good electrochemical performance. From galvanostatic charge-discharge studies, the compounds $LiNi_{0.7}Co_{.3}VO_4$ and $LiNi_{0.7}Mg_{0.3}VO_4$ that exhibited better cyclability and capacity over the parent $LiNiVO_4$ have been found to be acceptable for lithium battery purposes in the window of operation of 4.4V when coupled with proper choice non-aqueous electrolytes. Nevertheless, these compounds need research critically oriented towards issues such as selection of dopants, doping level from the lowest possible limit, fixing a nominal charge/discharge voltage limit, selection of organic electrolyte combination etc.

References

1. T. Nagaura, K. Tozawa, *Prog. Batteries Solar Cells,* 9 (1990) 209.
2. J.M. Tarascon, D. Guyomard, *J. Electrochem. Soc.,* 138 (1991) 2864.
3. J.R. Dahn , V. Von Sacken, M.W. Juzkow, H. Al-Janaby, *J. Electrochem. Soc,.* 138 (1991) 2207.
4. T. Ohzuku, A Ueda, M. Nagayama, *J. Electrochem. Soc,.* 140(1993) 1862
5. T. Ohzuku, H. Komori, K. Sawai, T. Hirai, *Chem. Express,* 5 (1990) 733
6. J.R. Dahn, E.W. Fuller, M. Obrovac and U. Von Sacken, *Solid State Ionic,s* 69(1994) 265
7. Ph. D dissertation of P. Kalyani, Faculty of Industrial Chemistry, Alagappa University, Karaikudi (India), 2003.
8. G.T.K. Fey, W. Li , J.R. Dahn, *J. Electrochem. Soc*., 141 (1994) 2279: G. T. K. Fey, W. B. Perng, Mat. Chem. Phy. 47 (1997) 279.
9. S.R.S. Prabaharan, M. S. Michael, S. Radhakrishnan, C. Julien, *J. Mater. Chem*., 7 (1997) 1791.
10. P. Kalyani, R. Jagannathan, S. Gopukumar, Chung-Hsin Lu, *Journal of Power Sources*, 109 (2002) 301

11. P Kalyani, S Sivasubramanian, S. Naveen Prabhu, K Ragavendran, N Kalaiselvi, N G Ranganathan, S Madhu, A.SundaraRaj, S P Manoharan and R Jagannathan1, J. *Phys. D: Appl. Phys.*, 38 (2005) 990
12. S. Panero. P. Reale, F. Bonino, B. Scrosati, M. Arrabito, S. Bodoardo, D. Mazza, N. Penazzi, *Solid State Ionics*, 128 (2000) 43.
13. Q.Y. Lai, J.Z. Lu, X.B. Su, X.Y.Ji, *J. Solid State Chem*., 165 (2002) 312.
14. P. Kalyani, N. Kalaiselvi & N. Muniyandi, *Mater. Chem. Phys.,* 77 (2002) 662
15. P. Kalyani, N. Kalaiselvi & N Muniyandi, *J. Power Sources*,111 (2002) 232
16. S. Chitra, P. Kalyani, B. Yebka, T. Mohan, E. Haro-Poniatowski, R. Gangadharan, C. Julien, *Mater. Chem. Phys*., 65 (2000) 32.
17. K. Nakamoto, Infrared and Raman Spectra of Inorganic and Coordination Compounds, 4th ed., John Wiley, USA, 1986.].
18. J. Preudhomme, P. Tarte, *Spectrochim. Acta*, 28A (1972) 69.